photochem

MDPI

Article

Antibacterial Activity of In Situ Generated Silver Nanoparticles in Hybrid Silica Films

Sudipto Pal [1,*], Rossella Nisi [2] and Antonio Licciulli [1,3]

[1] Department of Engineering for Innovation, University of Salento, Via per Monteroni, 73100 Lecce, Italy; antonio.licciulli@unisalento.it
[2] Biofaber Srl, Via Luigi di Savoia, 19, 72023 Mesagne, Italy; nisirossella@gmail.com
[3] Institute of Nanotechnology, CNR Nanotec, Consiglio Nazionale Delle Ricerche, Via Monteroni, 73100 Lecce, Italy
* Correspondence: sudipto.pal@unisalento.it

Abstract: Herein we present silver nanoparticles (AgNPs)-doped inorganic–organic hybrid silica films on glass and polypropylene substrates. A hybrid inorganic–organic silica sol in alcoholic medium was prepared at room temperature using TEOS, GLYMO, and APTES. Silver nanoparticles were generated in situ within the hybrid silica sol. AgNPs-SiO_2 film was obtained by dip coating method following drying at 80 °C. FTIR spectra shows several vibrational bands of the hybrid silica network and amine functionalization. AgNPs formation was observed from the XRD spectra of the dried film. UV–Visible spectra show sharp surface plasmon resonance (SPR) band centered at 412 nm arising from the evenly distributed silver nanoparticle inside the silica film that was supported by morphological characterization. Both the coated films showed good antibacterial activity against *E. coli* bacterial strain by forming a zone of inhibition in the agar diffusion test. The antibacterial efficiency for coated glass and polypropylene was 72.5% and 83.75%. This coating approach provides a straight-forward solution to prepare antibacterial coatings on various substrates especially on plastics, where low temperature processing is necessary.

Keywords: silver nanoparticles; sol-gel coating; hybrid silica film; antibacterial

Citation: Pal, S.; Nisi, R.; Licciulli, A. Antibacterial Activity of In Situ Generated Silver Nanoparticles in Hybrid Silica Films. *Photochem* **2022**, *2*, 479–488. https://doi.org/10.3390/photochem2030033

Academic Editor: Ewa Kowalska

Received: 1 May 2022
Accepted: 21 June 2022
Published: 23 June 2022

1. Introduction

The outbreak due to the super spreader and highly infectious coronavirus (SARS-CoV-2) has revealed the need to develop antibacterial and antiviral coating materials [1]. In particular, high-touch surfaces such as public transport, door handles, elevator keys, and other common areas in hospitals and offices are at high risk of spreading the airborne pathogens [2]. Silver has been used as a potent antimicrobial agent since ancient times [3,4]. Silver nanoparticles (AgNPs) are considered very potent antimicrobial/antifungal agents due to their strong cytotoxic effect toward a broad range of microorganism and remarkably low human toxicity compared to other heavy metals [5]. Although the actual reason for the antibacterial activity of AgNPs is not clear, many reports propose that Ag ions are released from the AgNPs, which strongly binds to the thiol groups present in the bacterial/microbial cell membrane and thus destroy the cell by puncturing the wall leading to cell death [5,6]. Many researchers have proposed several synthesis procedures to prepare highly antibacterial silver nanomaterials [5,7–12]. AgNPs have been successfully loaded on various porous supports to enhance the antimicrobial efficiency; Yang et al. described *E. coli* inactivation by AgNPs anchored on titania nanotubes [13], Joarder et al. reported enhanced antibacterial activity of AgNPs deposited on MCM-41 type mesoporous silica [14], Guo et al. described sustained release behavior of halloysite nanotubes loaded with the AgNPs [15], Dung et al. fabricated silver-doped ceramic filter for antimicrobial water purification [16], and Chen et al. reviewed the antibacterial activity of silver doped polymeric nanostructures [17]. However, it is necessary to achieve a proper antimicrobial coating that can be applied to

a variety of substrates since bare or supported AgNPs could exhibit some adverse effects due to excessive leaching in moist environments that could lead to diminished antibacterial activity and make the environment toxic as well [18–20]. Antimicrobial coatings based on AgNPs have been used in medical implants, biomedical devices, and in packaging material to inhibit the bacterial infection [3,21–25]. Most of the reported works describe either high temperature sintering or complex multistep procedures that might show difficulties in obtaining antibacterial coatings on a large scale [3,22,25].

In this work, we report one-pot synthesis of in situ generated AgNPs in organically modified hybrid silica films coated on glass and polypropylene substrates without using any additional reducing agents. Hybrid silica films show many advantageous properties compared to their inorganic counterpart due to their flexibility and film adherence on a range of substrates without crack formation when comparatively thicker coating is required [26–28]. They serve as excellent host for trapping and uniformly dispersing the metal and semiconductor nanoparticles because of their ability to act as stabilizers that terminates further growth of the nanoparticles by controlling the nucleation process [29,30]. AgNPs were generated inside the hybrid silica film during the synthesis process and coatings were deposited on glass slide and polypropylene sheets by the dip coating method. The films were characterized by UV–Visible spectroscopy, Fourier transform infrared spectroscopy (FTIR), X-ray diffraction (XRD) analysis, and scanning electron microscopy (SEM). The antibacterial activity of the coated films was tested against Gram negative *Escherichia coli* (*E. coli*) bacterial strain.

2. Materials and Methods

2.1. Chemicals and Biological Reagents

All the chemicals in the synthesis procedure were used without any modification. Tetraethylorthisilicate (TEOS, Sigma-Aldrich, St. Luis, MO, USA, Reagent grade, 98%) was used as inorganic precursor, and (3-Glycidyloxypropyl)triethoxysilane (GLYMO, Sigma-Aldrich, ≥98%) and (3-Aminopropyl)triethoxysilane (APTES, Sigma-Aldrich, ≥98%) were used as the organic precursors of silica. Silver nitrate ($AgNO_3$, Alfa Aesar Gmbh & Co KG, Karlsruhe, Germany, 99+%) was used as the silver source. Agar powder was purchased from A.C.E.F., Luria-Bertani (LB) broth (Miller) and *E coli* culture BL21 (DE3) strain were purchased from Merck KGaA, Germany. Milli Q ultrapure water (Resistivity 18.2 MΩ cm) was used throughout the experimental procedure.

2.2. Hybrid AgNPs-SiO_2 Film Preparation

Inorganic–organic hybrid coating approach was followed to prepare the AgNPs-SiO_2 coatings on glass slides and PP sheets. Ag nanoparticles were generated inside the SiO_2 film matrix at sol processing stage. This inorganic–organic hybrid coating approach not only helps to induce the formation of AgNPs inside the SiO_2 film, but also increases the adherence to the polypropylene sheets, which was not achieved from conventional silica sol. In addition, 10 equivalent wt% of SiO_2 was maintained to produce a thicker coating without suffering the cracking and 5 mol% of Ag with respect to SiO_2 was used as the dopant. The molar composition of TEOS: GLYMO: APTES was maintained at 6:3:1 and 1.5 mole of H_2O and 10^{-2} mole of HNO_3 per mole of the alkoxide group was used in the sol to initiate the hydrolysis-condensation reaction, while 2-propanol was used as the solvent. First, the hybrid silica sol was prepared and kept in a closed container for one day. Then, the required amount of $AgNO_3$ dissolved in a little amount of water was mixed with stirring. After 10 min of stirring, the color of the sol changed gradually to dark brown indicating the formation of AgNPs in the sol. Cleaned glass slides and polypropylene sheets were coated with the above sol by dip coating method using the lifting speed of 20 cm/min. After coating deposition, the coated substrates were kept in an oven at 80 °C overnight to densify the coating. The coated films showed uniform bright yellow color, which indicates that AgNPs have been formed inside the silica film. The schematic diagram of the film forming process is presented in Figure 1.

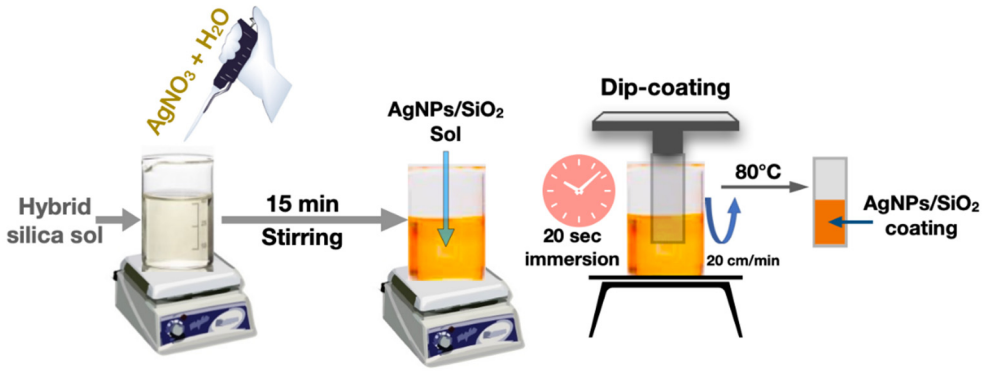

Figure 1. Schematic diagram of the AgNPs/SiO_2 film formation by dip coating method.

2.3. Characterizations

Nanocrystalline nature of the AgNPs in silica film on glass and polypropylene substrates was characterized by X-ray diffraction (XRD) measurement, performed on a Rigaku Ultima X-ray diffractometer using CuK_α radiation (λ = 1.5406 Å) operating at 40 kV/30 mA with the step size of 0.02°. FTIR spectra of the dried film were recorded with a JASCO FTIR-6300 instrument over the range 4000–400 cm^{-1} with a resolution of 4 cm^{-1} by accumulating 256 scans for each measurement, adopting the KBr disc method. A little amount of the film was scrapped off from the coated glass substrate and mixed with the KBr (powder: KBr weight ratio of 1:10) to prepare the IR transparent disk. UV–Visible absorption spectra of the films coated on glass and polypropylene were measured with Agilent Cary 5000 UV–Visible–NIR spectrophotometer. The coated glass slides and PP sheets were fixed to the solid sample holder accessory and mounted into the sample compartment in transmission mode. Uncoated glass slide and PP sheet were used as reference material while performing baseline correction. The absorption spectra were measured directly from the drop-down measurement command (Absorbance) in the software. Morphology of the AgNPs-SiO_2 film was observed with a Zeiss (model Sigma VP) field emission scanning electron microscope (FESEM).

2.4. Assay of Antimicrobial Activity

The antimicrobial activity of AgNPs-SiO_2 coated glass slide and polypropylene sheet was investigated against the common pathogenic bacteria *E. coli* as the model microorganism, which was pre-cultured at 37 °C to reach a concentration above 10^8 colony forming units (CFU/mL). The turbidity assay was performed to quantitatively evaluate the antimicrobial activity by observing the optical density of the strain at 600 nm. Each sample was added into 25 mL of *E. coli*. nutrient broth, seeded with 0.05 mL of test strains (1.6–1.9 × 10^8 CFU of total bacteria number), and incubated at 37 °C for 18 h. Different dilutions of the bacterial suspensions were then transferred onto nutrient agar plates and incubated at 37 °C for 18 h. After that, the viable bacteria were monitored by counting the number of colony forming units from the appropriate dilution on nutrient agar plates and expressed as CFU. The same procedure was performed on bare substrates as control.

3. Results and Discussion

Silver nanoparticles were generated in the inorganic–organic hybrid silica matrix without using any additional reducing agent. Here, APTES played a crucial role to reduce Ag^+ to Ag^0. Choi et al. reported that aminosilane could be utilized to produce metallic silver nanoparticles embedded in sol-gel silica matrix without using any external reducing precursor [30]. Therefore, we can assume that the amine functional groups originating from APTES could reduce $AgNO_3$ to form Ag nanoparticles in the hybrid silica matrix in presence of water. The reduction process was monitored by observing the sol color change from colorless sol to light brownish to deep brown. The amine functionalization to the silica matrix and the formation of SiO_2 network was investigated by FTIR measurements,

which is presented in Figure 2. The most informative region is situated in the wavenumber range between 946 to 1250 cm^{-1} due to the Si−O−Si network, where the most intense band is observed that consists of a group of bands. The characteristics of this band are quite different than those reported for inorganic–organic hybrid silica film, where a relatively sharp band has been shown [26,31]. The vibrational bands centered at 1092 and 805 cm^{-1} are assigned to the asymmetric and symmetric stretching of Si−O−Si, respectively [26,32]. The Si−O−Si asymmetric stretching band is overlapped with the Si−O−C vibrational band. A peak due to the NO^{-3} group at 1387 cm^{-1} is also observed indicating the presence of nitrates inside the film originating from silver nitrate [31]. Absence of the epoxide bands at 1260–1240 cm^{-1} (epoxy ring breathing) and 950–810 cm^{-1} (asymmetrical ring stretching) indicate the polymerization of epoxide groups [31]. The broad band around 3300–3600 cm^{-1} and relatively low intense band at 976 cm^{-1} are attributed to the stretching vibration of H-bonded silanols (Si−OH) with hydroxyl groups of the adsorbed water molecules. Interestingly, there are new bands centered at 1035 and 1150 cm^{-1}, which are assigned to Si−O−Si transverse optical (TO) and Si−O−Si longitudinal optical (LO) stretching modes, respectively (Figure 2), which strongly suggest the functionalization of APTES with the silica network [33,34]. This functionalization is further confirmed by the appearance of CH_3 asymmetric mode at 2975 cm^{-1} and CH_2 asymmetric and symmetric stretching modes at 2931 and 2865 cm^{-1} [33]. There are also some low intense peaks between 1500 to 1600 cm^{-1} that could be assigned to the $-NH_2$ scissor vibration and asymmetric NH^{+}_3 deformation mode, both originating from APTES, which also support the APTES functionalization with the Si−O−Si.

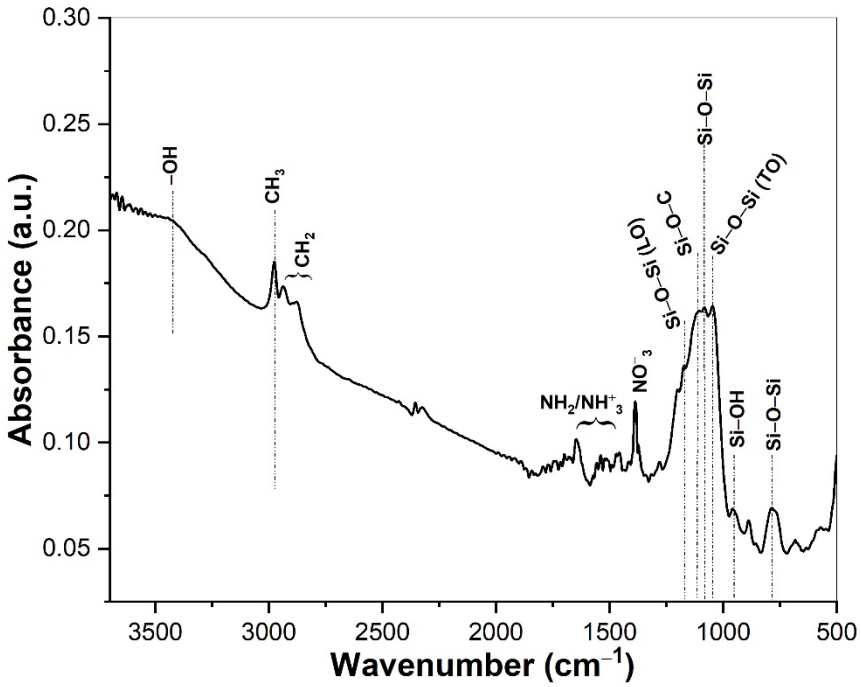

Figure 2. FTIR spectra of the AgNPs/SiO_2 film dried at 80 °C. Major peaks corresponding to each wavenumber are indicated in the figure.

Figure 3 shows the XRD pattern of the AgNPs/SiO_2 film coated on glass and polypropylene substrates dried at 80 °C. In both cases, low intensity and broad diffraction peaks appeared around 38.18° 2θ that correspond to the <111> plane of the face centered cubic crystalline phase of metallic silver [26]. The appearance of broader diffraction peaks indicates the formation of evenly distributed small sized-silver nanoclusters inside the silica film that is supported by the morphological investigation discussed later on. We did not observe any additional peaks due to the silver oxides [35].

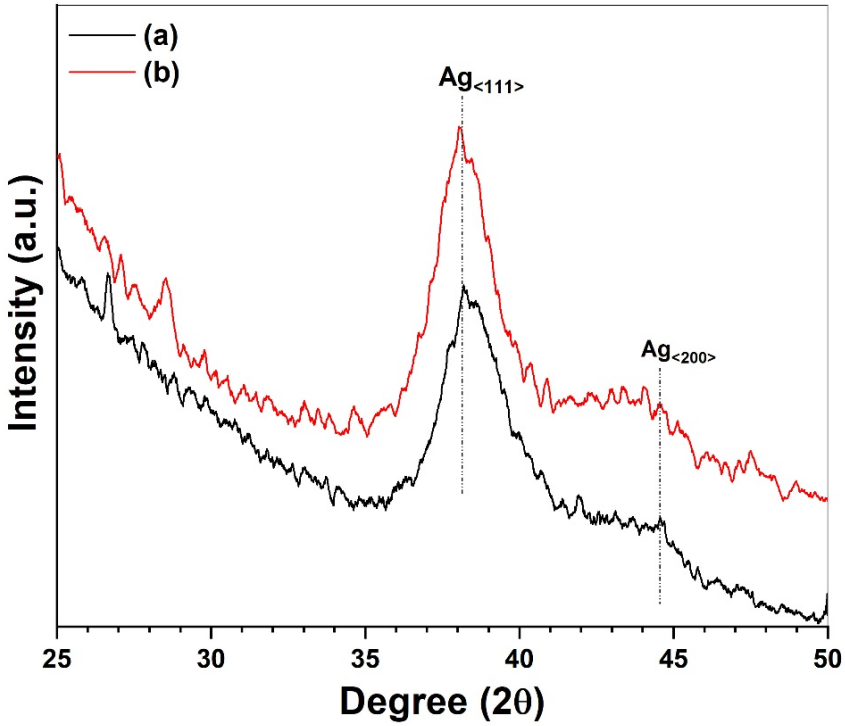

Figure 3. XRD pattern of AgNPs/SiO_2 film coated on (**a**) glass slide and (**b**) PP after drying at 80 °C.

UV–Visible absorption spectra of the AgNPs/SiO_2 coated films on glass slide and polypropylene sheet are presented in Figure 4. Both the films show a strong absorption band centered at 412 nm wavelength that can be explained by the surface plasmon resonance (SPR) band of the AgNPs. The appearance of sharp and intense SPR band without having any additional shoulder peaks at higher wavelength region strongly suggests the uniformly dispersed AgNPs throughout the silica film having narrow size distribution without forming any agglomeration [36]. This is also supported by the appearance of the bright yellow color of the coated films (inset of Figure 4).

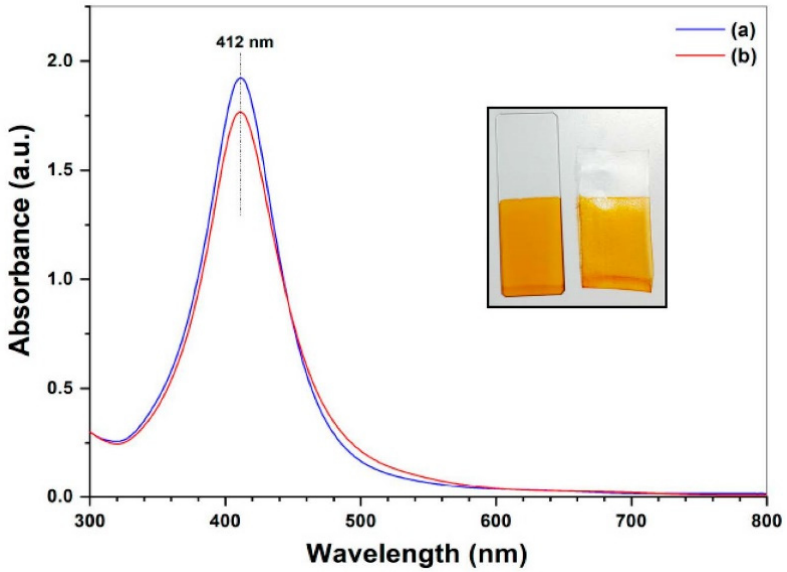

Figure 4. UV–Visible spectra of AgNPs/SiO_2 film coated on (**a**) glass slide and (**b**) PP sheet after drying at 80 °C. The inset shows real photograph of the AgNPs/SiO_2 coating on glass slide (left) and PP sheet (right) after drying.

The electron micrographs (FESEM) images of the AgNPs in silica film is shown in Figure 5 with different magnification (Figure 5a–c). It is clearly evidenced that the AgNPs are evenly distributed inside the silica film matrix. No distinguishable agglomeration was observed. The average size of the AgNPs was found to be about 20 nm (Figure 5d), which is in good agreement with the optical absorption spectra [36].

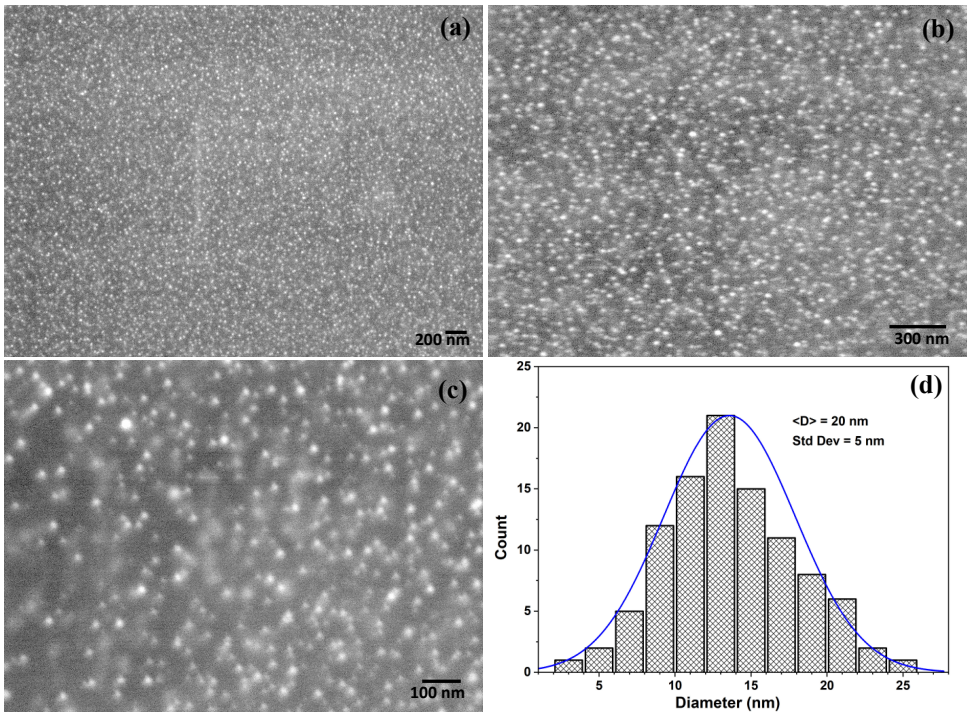

Figure 5. (**a**–**c**) SEM images of the AgNPs/SiO_2 film surface coated on glass substrates with different magnifications and (**d**) particles size distribution of the AgNPs counted from image (**c**) using Image J software.

Biocidal activity of the AgNPs-SiO_2 films coated on glass slides and polypropylene sheets were evaluated qualitatively and quantitatively against *E. coli*, which is the most commonly used Gram-negative food borne pathogen that is also present in lower intestinal tract of warm-blooded animals, including humans [37]. *E. coli* is often responsible for bacterial infection of the environment through fecal discharge and wastewater from sewage [38]. It is also easy to grow the *E. coli* very fast with diverse species in laboratory conditions (~37 °C) that is also well understood so far by several studies [37–39]. The qualitative evaluation was examined by observing the inhibition zone formation around the coated film using the disk diffusion method (Figure 6a,b). It is clearly visible from the figure that AgNPs/SiO_2 coated films inhibited the bacterial growth by forming a well resolved inhibition zone around the coated film that confirm no bacterial growth around the coating, whereas there was no evidence of inhibition zone formation in case of uncoated substrates that reveal no antibacterial activity of the uncoated substrates. It is also noticeable that the diameter of the inhibition zone is higher for polypropylene that the glass slides which suggests strong adherence of the AgNPs/SiO_2 film with the glassy surface that might control the release of Ag^+ ions, which are responsible for the killing of the bacteria. Since the glass surface has many hydroxyl groups (Si-OH) favoring the surface wettability, and AgNPs containing hybrid silica sol also have silanol groups, a strong chemical bonding could occur between the glass slide and the hybrid silica sol. On the other hand, polypropylene, having a chemical formula of $(C_3H_6)_n$, where the methyl groups (CH_3) are arranged on the carbon chain, shows strong hydrophobicity that makes it difficult to coat with only TEOS-derived silica sol. Although the inorganic–organic hybrid sol favored the film formation on PP substrate, it may lack the strong adherence achieved in case of the glass slides. The qualitative

antibacterial efficiency was obtained by the turbidity assay of the growth solution, where the optical absorption at 600 nm (OD_{600}) was recorded and expressed as colony forming unit (CFU). The antibacterial efficiency was calculated by the following equation [6]

$$\text{Efficiency} = [1 - CFU_{Ag}/CFU_0] \quad (1)$$

where CFU_{Ag} and CFU_0 represent the bacterial concentration with AgNPs/SiO_2 film and with uncoated substrates, respectively. Figure 6c shows the bacterial growth solution with AgNPs/SiO_2 coated glass and polypropylene substrates and a control solution after 18 h of incubation. The growth solution containing coated films show optically clear appearance compared to turbid appearance of the control solution indicating the coated film inhibited the *E. coli* growth. The antibacterial efficiency is presented in Figure 6d, where it is observed that 83.75% efficiency was obtained for the coated polypropylene substrate, whereas for the coated glass substrate it was 72.5%.

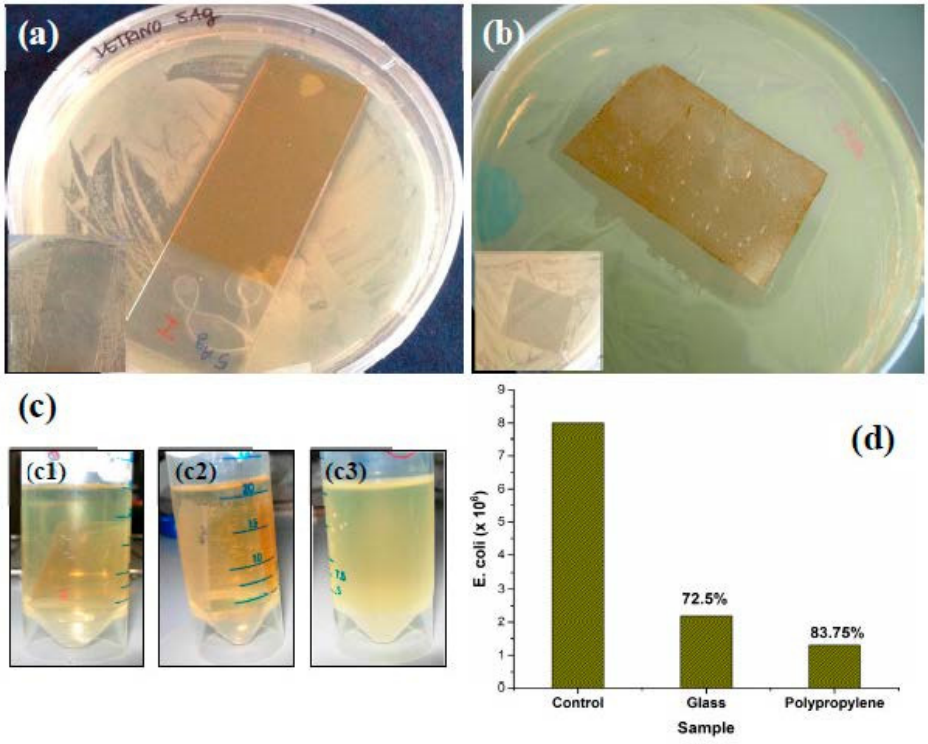

Figure 6. Antibacterial activity evaluation by inhibition zone formation with AgNPs/SiO_2 coated (**a**) glass and (**b**) polypropylene against *E. coli* bacterial strain. the inset shows the same with uncoated substrates. (**c**) Photographs of the *E. coli* strain with AgNPs/SiO_2 coated on glass (**c1**), polypropylene (**c2**), and control (**c3**). (**d**) *E. coli* cell number (CFU/mL) in growth solution with different coated substrate along with the calculated antibacterial efficiency.

Comparatively lower antibacterial efficiency of the glass slides is in agreement with the lower inhibition zone formation compared to the coated polypropylene sheets (Figure 6a,b). Similar antibacterial activities of the AgNPs dispersed in silica coating have been also reported [40–42].

4. Conclusions

In this work, we have reported a simple coating approach based on AgNPs in hybrid silica sol to effectively obtain biocide film on various substrates. Since the AgNPs are produced in situ inside the silica sol, it excludes the second step of reducing the Ag^+ to Ag^0, either by using a reducing agent or by thermal curing. The process could be interesting for low temperature curing substrate such as plastics and/or where a reduction step is difficult to carry out, e.g., common touch surfaces. AgNPs containing silica sol can also

be sprayed or rolled to coat larger substrates. Since the coated films showed moderate antibacterial activity (72.5% and 83.75% for glass and polypropylene), and the AgNPs are protected inside the glassy SiO_2 film, they could be potential candidate in food packaging industries, where there are limited chances of contamination due to silver leaching. We will investigate in detail how Ag^+ releases from the films on various substrates and its effect on the antibacterial activity.

Author Contributions: Conceptualization, S.P. and A.L.; methodology, S.P. and R.N.; investigation, S.P. and R.N.; software, S.P.; original draft preparation, S.P. and R.N.; review and editing, S.P. and A.L.; supervision, S.P. and A.L. All authors have read and agreed to the published version of the manuscript.

Funding: A part of the research work was funded by Biofaber Srl.

Institutional Review Board Statement: Not applicable.

Informed Consent Statement: Not applicable.

Data Availability Statement: Not applicable.

Acknowledgments: Authors thankfully acknowledge Fabio Marzo for providing the FESEM measurements and Donato Cannoletta for XRD measurements.

Conflicts of Interest: The authors declare no conflict of interest.

References

1. Ghezzi, S.; Pagani, I.; Poli, G.; Pal, S.; Licciulli, A.; Perboni, S.; Vicenzi, E. Rapid Inactivation of SARS-CoV-2 by Coupling Tungsten Trioxide (WO3) Photocatalyst with Copper Nanoclusters. *J. Nanotechnol. Nanomater.* **2020**, *1*, 109–115. [CrossRef]
2. Mitra, D.; Kang, E.-T.; Neoh, K.G. Antimicrobial Copper-Based Materials and Coatings: Potential Multifaceted Biomedical Applications. *ACS Appl. Mater. Interfaces* **2020**, *12*, 21159–21182. [CrossRef] [PubMed]
3. Zhou, Y.; Fletcher, N.F.; Zhang, N.; Hassan, J.; Gilchrist, M.D. Enhancement of Antiviral Effect of Plastic Film against SARS-CoV-2: Combining Nanomaterials and Nanopatterns with Scalability for Mass Manufacturing. *Nano Lett.* **2021**, *21*, 10149–10156. [CrossRef] [PubMed]
4. Pal, S.; Nisi, R.; Stoppa, M.; Licciulli, A. Silver-Functionalized Bacterial Cellulose as Antibacterial Membrane for Wound-Healing Applications. *ACS Omega* **2017**, *2*, 3632–3639. [CrossRef]
5. Chen, S.-S.; Xu, H.; Xu, H.-J.; Yu, G.-J.; Gong, X.-L.; Fang, Q.-L.; Leung, K.C.-F.; Xuan, S.-H.; Xiong, Q.-R. A Facile Ultrasonication Assisted Method for Fe_3O_4@SiO_2-Ag Nanospheres with Excellent Antibacterial Activity. *Dalton Trans.* **2015**, *44*, 9140–9148. [CrossRef]
6. Ko, Y.-S.; Joe, Y.H.; Seo, M.; Lim, K.; Hwang, J.; Woo, K. Prompt and Synergistic Antibacterial Activity of Silver Nanoparticle-Decorated Silica Hybrid Particles on Air Filtration. *J. Mater. Chem. B* **2014**, *2*, 6714–6722. [CrossRef]
7. Fernández, E.J.; García-Barrasa, J.; Laguna, A.; López-de-Luzuriaga, J.M.; Monge, M.; Torres, C. The Preparation of Highly Active Antimicrobial Silver Nanoparticles by an Organometallic Approach. *Nanotechnology* **2008**, *19*, 185602. [CrossRef]
8. Mosselhy, D.A.; Granbohm, H.; Hynönen, U.; Ge, Y.; Palva, A.; Nordström, K.; Hannula, S.-P. Nanosilver–Silica Composite: Prolonged Antibacterial Effects and Bacterial Interaction Mechanisms for Wound Dressings. *Nanomaterials* **2017**, *7*, 261. [CrossRef]
9. Pavoski, G.; Kalikoski, R.; Souza, G.; Brum, L.F.W.; dos Santos, C.; Abo Markeb, A.; dos Santos, J.H.Z.; Font, X.; dell'Erba, I.; Galland, G.B. Synthesis of Polyethylene/Silica-Silver Nanocomposites with Antibacterial Properties by in Situ Polymerization. *Eur. Polym. J.* **2018**, *106*, 92–101. [CrossRef]
10. Abduraimova, A.; Molkenova, A.; Duisembekova, A.; Mulikova, T.; Kanayeva, D.; Atabaev, T.S. Cetyltrimethylammonium Bromide (CTAB)-Loaded SiO_2–Ag Mesoporous Nanocomposite as an Efficient Antibacterial Agent. *Nanomaterials* **2021**, *11*, 477. [CrossRef]
11. Wan, M.; Zhao, H.; Peng, L.; Zhao, Y.; Sun, L. Facile One-Step Deposition of Ag Nanoparticles on SiO_2 Electrospun Nanofiber Surfaces for Label-Free SERS Detection and Antibacterial Dressing. *ACS Appl. Bio Mater.* **2021**, *4*, 6549–6557. [CrossRef]
12. Gonzalo-Juan, I.; Xie, F.; Becker, M.; Tulyaganov, D.U.; Ionescu, E.; Lauterbach, S.; De Angelis Rigotti, F.; Fischer, A.; Riedel, R. Synthesis of Silver Modified Bioactive Glassy Materials with Antibacterial Properties via Facile and Low-Temperature Route. *Materials* **2020**, *13*, 5115. [CrossRef] [PubMed]
13. Yang, C.; Jian, R.; Huang, K.; Wang, Q.; Feng, B. Antibacterial Mechanism for Inactivation of E. Coli by AgNPs@polydoamine/Titania Nanotubes via Speciation Analysis of Silver Ions and Silver Nanoparticles by Cation Exchange Reaction. *Microchem. J.* **2021**, *160*, 105636. [CrossRef]
14. Joardar, S.; Adams, M.L.; Biswas, R.; Deodhar, G.V.; Metzger, K.E.; Deweese, K.; Davidson, M.; Richards, R.M.; Trewyn, B.G.; Biswas, P. Direct Synthesis of Silver Nanoparticles Modified Spherical Mesoporous Silica as Efficient Antibacterial Materials. *Microporous Mesoporous Mater.* **2021**, *313*, 110824. [CrossRef]

15. Guo, W.; Liu, W.; Xu, L.; Feng, P.; Zhang, Y.; Yang, W.; Shuai, C. Halloysite Nanotubes Loaded with Nano Silver for the Sustained-Release of Antibacterial Polymer Nanocomposite Scaffolds. *J. Mater. Sci. Technol.* **2020**, *46*, 237–247. [CrossRef]
16. Ngoc Dung, T.T.; Phan Thi, L.-A.; Nam, V.N.; Nhan, T.T.; Quang, D.V. Preparation of Silver Nanoparticle-Containing Ceramic Filter by in-Situ Reduction and Application for Water Disinfection. *J. Environ. Chem. Eng.* **2019**, *7*, 103176. [CrossRef]
17. Chen, J.; Wang, F.; Liu, Q.; Du, J. Antibacterial Polymeric Nanostructures for Biomedical Applications. *Chem. Commun.* **2014**, *50*, 14482–14493. [CrossRef]
18. Ferdous, Z.; Nemmar, A. Health Impact of Silver Nanoparticles: A Review of the Biodistribution and Toxicity Following Various Routes of Exposure. *Int. J. Mol. Sci.* **2020**, *21*, 2375. [CrossRef]
19. Gankhuyag, S.; Bae, D.S.; Lee, K.; Lee, S. One-Pot Synthesis of SiO_2@Ag Mesoporous Nanoparticle Coating for Inhibition of Escherichia Coli Bacteria on Various Surfaces. *Nanomaterials* **2021**, *11*, 549. [CrossRef]
20. Kakakhel, M.A.; Wu, F.; Sajjad, W.; Zhang, Q.; Khan, I.; Ullah, K.; Wang, W. Long-Term Exposure to High-Concentration Silver Nanoparticles Induced Toxicity, Fatality, Bioaccumulation, and Histological Alteration in Fish (Cyprinus Carpio). *Environ. Sci. Eur.* **2021**, *33*, 14. [CrossRef]
21. Catalano, P.N.; Pezzoni, M.; Costa, C.; Soler-Illia, G.J.d.A.A.; Bellino, M.G.; Desimone, M.F. Optically Transparent Silver-Loaded Mesoporous Thin Film Coating with Long-Lasting Antibacterial Activity. *Microporous Mesoporous Mater.* **2016**, *236*, 158–166. [CrossRef]
22. Mukhopadhyay, A.; Basak, S.; Das, J.K.; Medda, S.K.; Chattopadhyay, K.; De, G. Ag−TiO_2 Nanoparticle Codoped SiO_2 Films on ZrO_2 Barrier-Coated Glass Substrates with Antibacterial Activity in Ambient Condition. *ACS Appl. Mater. Interfaces* **2010**, *2*, 2540–2546. [CrossRef] [PubMed]
23. Marini, M.; De Niederhausern, S.; Iseppi, R.; Bondi, M.; Sabia, C.; Toselli, M.; Pilati, F. Antibacterial Activity of Plastics Coated with Silver-Doped Organic−Inorganic Hybrid Coatings Prepared by Sol−Gel Processes. *Biomacromolecules* **2007**, *8*, 1246–1254. [CrossRef] [PubMed]
24. Shen, Q.; Shan, Y.; Lü, Y.; Xue, P.; Liu, Y.; Liu, X. Enhanced Antibacterial Activity of Poly (Dimethylsiloxane) Membranes by Incorporating SiO_2 Microspheres Generated Silver Nanoparticles. *Nanomaterials* **2019**, *9*, 705. [CrossRef]
25. Soule, L.D.; Pajares Chomorro, N.; Chuong, K.; Mellott, N.; Hammer, N.; Hankenson, K.D.; Chatzistavrou, X. Sol–Gel-Derived Bioactive and Antibacterial Multi-Component Thin Films by the Spin-Coating Technique. *ACS Biomater. Sci. Eng.* **2020**, *6*, 5549–5562. [CrossRef]
26. Pal, S.; De, G. A New Approach for the Synthesis of Au−Ag Alloy Nanoparticle Incorporated SiO_2 Films. *Chem. Mater.* **2005**, *17*, 6161–6166. [CrossRef]
27. De, G.; Medda, S.K.; De, S.; Pal, S. Metal Nanoparticle Doped Coloured Coatings on Glasses and Plastics through Tuning of Surface Plasmon Band Position. *Bull. Mater. Sci.* **2008**, *31*, 479–485. [CrossRef]
28. Medda, S.K.; Mitra, M.; De, S.; Pal, S.; De, G. Metal Nanoparticle-Doped Coloured Films on Glass and Polycarbonate Substrates. *Pramana* **2005**, *65*, 931–936. [CrossRef]
29. Hah, H.J.; Koo, S.M.; Lee, S.H. Preparation of Silver Nanoparticles through Alcohol Reduction with Organoalkoxysilanes. *J. Sol-Gel Sci. Technol.* **2003**, *26*, 467–471. [CrossRef]
30. Choi, Y.-J.; Huh, U.; Luo, T.-J.M. Spontaneous Formation of Silver Nanoparticles in Aminosilica. *J. Sol-Gel Sci. Technol.* **2009**, *51*, 124–132. [CrossRef]
31. De, S.; De, G. Coarsening of Ag Nanoparticles in SiO_2–PEO Hybrid Film Matrix by UV Light. *J. Mater. Chem.* **2006**, *16*, 3193–3198. [CrossRef]
32. Liciulli, A.; Nisi, R.; Pal, S.; Laera, A.M.; Creti, P.; Chiechi, A. Photo-Oxidation of Ethylene over Mesoporous Tio2/Sio2 Catalysts. *Adv. Hortic. Sci.* **2016**, *30*, 75–80. [CrossRef]
33. Pasternack, R.M.; Rivillon Amy, S.; Chabal, Y.J. Attachment of 3-(Aminopropyl)Triethoxysilane on Silicon Oxide Surfaces: Dependence on Solution Temperature. *Langmuir* **2008**, *24*, 12963–12971. [CrossRef] [PubMed]
34. Zhang, D.; Hegab, H.E.; Lvov, Y.; Dale Snow, L.; Palmer, J. Immobilization of Cellulase on a Silica Gel Substrate Modified Using a 3-APTES Self-Assembled Monolayer. *SpringerPlus* **2016**, *5*, 48. [CrossRef]
35. Pal, S.; De, G. Reversible Transformations of Silver Oxide and Metallic Silver Nanoparticles inside SiO_2 Films. *Mater. Res. Bull.* **2009**, *44*, 355–359. [CrossRef]
36. Kumar, A.; Goia, D.V. Preparation of Concentrated Stabilizer-Free Dispersions of Uniform Silver Nanoparticles. *Polyhedron* **2022**, *219*, 115804. [CrossRef]
37. Price, R.G.; Wildeboer, D. *E. coli as an Indicator of Contamination and Health Risk in Environmental Waters*; IntechOpen: London, UK, 2017; ISBN 978-953-51-3330-8.
38. Jang, J.; Hur, H.-G.; Sadowsky, M.j.; Byappanahalli, M.n.; Yan, T.; Ishii, S. Environmental Escherichia Coli: Ecology and Public Health Implications—A Review. *J. Appl. Microbiol.* **2017**, *123*, 570–581. [CrossRef]
39. Cronan, J.E. Escherichia Coli as an Experimental Organism. In *eLS*; John Wiley & Sons, Ltd.: Hoboken, NJ, USA, 2014; ISBN 978-0-470-01590-2.
40. Toker, R.D.; Kayaman-Apohan, N.; Kahraman, M.V. UV-Curable Nano-Silver Containing Polyurethane Based Organic–Inorganic Hybrid Coatings. *Prog. Org. Coat.* **2013**, *76*, 1243–1250. [CrossRef]

41. Miola, M.; Perero, S.; Ferraris, S.; Battiato, A.; Manfredotti, C.; Vittone, E.; Del Vento, D.; Vada, S.; Fucale, G.; Ferraris, M. Silver Nanocluster-Silica Composite Antibacterial Coatings for Materials to Be Used in Mobile Telephones. *Appl. Surf. Sci.* **2014**, *313*, 107–115. [CrossRef]
42. Procaccini, R.A.; Studdert, C.A.; Pellice, S.A. Silver Doped Silica-Methyl Hybrid Coatings. Structural Evolution and Antibacterial Properties. *Surf. Coat. Technol.* **2014**, *244*, 92–97. [CrossRef]